Hybrid Beamforming: Reduced Eigen Beamforming on Beam Signals

Ingo Viering, Thomas Frey, Gottfried Schnabl
Siemens AG, Lise-Meitner-Strasse 7, 89081 Ulm
{Ingo.Viering.GP, Thomas.Frey, Gottfried.Schnabl}@icn.siemens.de

Abstract— **A hybrid beamforming technique for multiple antenna receivers is introduced. It is a combination of a simple fixed beam method and the adaptive eigen beamforming algorithm. This two-stage solution allows for a user-specific scalable trade-off between performance and complexity, depending on the interference scenario. Furthermore, the dimensions of the eigen beamforming stage can be reduced with only slight performance degradation. The hybrid scheme is compared with the stand-alone algorithms in different 2-user scenarios under ideal as well as under more realistic assumptions. It is shown, that in many scenarios the fixed beamforming stage is sufficient. In more severe interference scenarios, the hybrid techniques approaches the performance of the eigen beamformer with less complexity.**

Keywords— **Beamforming, Eigen Beamforming, Fixed Beamforming, Spatial Signal Processing, Dimension Reduction**

I. Introduction

BEAMFORMING is a promising technique to improve both capacity and coverage in mobile communication systems. The latter exploits the antenna gain to extend the cell sizes, which is an important feature especially concerning the initial roll-out of new systems such as UMTS. The capacity is enhanced by forming adaptive beam patterns which suppress the interference power.

Efficient algorithms are needed, which are capable to adapt to the spatial interference situation. On the other hand, complexity is a very important issue. A lot of methods have been proposed in the past, however, the complexity is often very high when considering current receiver structures.

The *eigen beamformer* [1] maximizes the signal to interference and noise ratio (SINR) for each user and for any spatial configuration. Since the beamforming and the weight calculations are done user-specific, the complexity is still high. One of the simplest possibilities is to form a number of static beams in different directions to cover the whole sector of interest. This *fixed beamforming* [2] is done only once for all users. For each user, the best beam signals are selected and maximum ratio combined. However, the adaptivity is low for some scenarios.

This paper describes a novel hybrid method which combines both algorithms. Here, the eigen beamformer operates on the beam signals generated by a fixed beamforming network rather than on the aperture signals.

For the sake of convenience, most considerations throughout this article are made for frequency-non-selective channels, i.e. with no multipath dispersion present. Similar to [1] the insights are easily extended to the frequency-selective case by repeating the operations for each channel tap. The results in section V consider frequency-selective channels.

Furthermore, the wide sense stationarity (WSS) assumption is used, i.e. the environment is assumed to be constant for a certain time interval. In other words, fast-fading is considered, but not slow-fading.

The structure is as follows: section II describes the concepts of the eigen beamformer, the fixed beamformer and the novel hybrid beamformer. Section III introduces the simulation scenarios and parameters which are used in section IV to analyze and to compare the three methods under ideal assumptions. More realistic simulation results are presented in section V. Finally, the main aspects of this work are summarized in section VI.

Throughout this paper, matrices (e.g. $\mathbf{R}$) are written in capital bold letters, vectors (e.g. $\vec{r}$) in small letters with an arrow, $\mathbf{E}\{\}$ is the expectation, and the superscript ^{H} denotes the conjugate transpose of a vector or a matrix, respectively.

II. Beamforming Receiver Concepts

Figure 1 depicts the conceptual structure for a beamforming unit of a multiple antenna receiver.

The antenna array receives a $K_a \times 1$ vector signal $\vec{r}(t)$, where

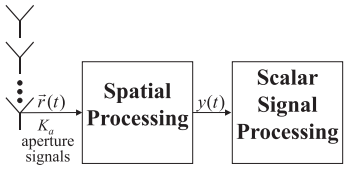

Fig. 1. General Beamformer Receiver Structure

K_a is the number of antennas and the elements of $\vec{r}(t)$ are the aperture signals. The received vector signal includes the desired vector signal $\vec{x}(t)$ and some vector perturbation $\vec{n}(t)$ corrupting the desired signal. The latter might be arbitrary interferer signals and/or thermal receiver noise [1]. In the sequel this perturbation is denoted as noise, although it contains also interference components.

$$\vec{r}(t) = \vec{x}(t) + \vec{n}(t) \tag{1}$$

Signal $\vec{x}(t)$ and noise $\vec{n}(t)$ are assumed to be mutually uncorrelated. However, the element signals in $\vec{x}(t)$ and $\vec{n}(t)$ are in general spatially correlated. These correlations are expressed in the spatial covariance matrices

$$\mathbf{R}_{xx} = \mathbf{E}\{\vec{x}(t) \cdot \vec{x}(t)^H\} \quad ; \quad \mathbf{R}_{nn} = \mathbf{E}\{\vec{n}(t) \cdot \vec{n}(t)^H\} \tag{2}$$

These correlations depend in particular on the angular spread of the impinging signals. A wide angular spread means low correlations and vice versa. An angular spread of 0^o, i.e. a single

[1] The receiver noise superimposes in the RF part of the receiver. For the sake of convenience, it is included in the antenna signals here

discrete direction, translates to total correlations.
The general task of the spatial processing in figure 1 is to combine the vector signal $\vec{r}(t)$ to a scalar signal $y(t)$ where the desired signal should be maximized and the noise should be minimized. The scalar signal $y(t)$ is then fed into following scalar signal processing units, which might be for instance despreading, channel decoding or bit decision, depending on the system properties.
Maximum ratio combining (MRC) maximizes the SNR [3] in the presence of uncorrelated noise, i.e. for a diagonal structure of $\mathbf{R}_{nn}$.
For an arbitrary structure of $\mathbf{R}_{nn}$, the Wiener solution [4] maximizes the SINR.
In the case of correlated desired signals $\vec{x}(t)$, i.e. a non-diagonal structure of $\mathbf{R}_{xx}$, the correlations can be exploited resulting in a dimension reduction of the signal space which in turn simplifies the MRC or the Wiener solution, respectively. This is utilized by the eigen beamformer.

A. Eigen Beamformer

Figure 3 shows the structure of the eigen beamformer [1].
The received signal $\vec{r}(t)$ is used to estimate the spatial covariance matrices of the desired signal and the noise $\mathbf{R}_{xx}$ and $\mathbf{R}_{nn}$. A generalized eigen value decomposition (EVD) is applied to the covariance matrices. All eigen vectors are used to transform the received signals $\vec{r}(t)$ from the K_a-dimensional aperture domain into the K_a-dimensional eigen domain.

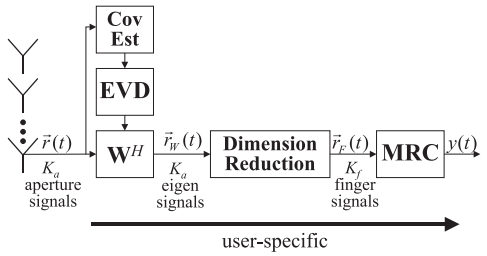

Fig. 2. Eigen Beamformer Receiver Structure

The resulting *eigen signals* $\vec{r}_W(t)$ have two important properties:

1. Both the signal and the noise components in the transformed signals $\vec{r}_W(t)$ are uncorrelated.
2. The SINR is not constant over the transformed signals, but it occurs concentrated.

The consequence of the first property is, that now MRC is used to combine the eigen signals $\vec{r}_W(t)$ to the signal $y(t)$. Moreover, due to the SINR concentration, the signal space can be reduced, i.e. a K_f-dimensional subset of the K_a eigen signals is usually sufficient to describe the complete signal space. The more correlated the aperture signals $\vec{r}(t)$ are, the larger is the dimension reduction, e.g. a single discrete direction spans a 1-dimensional signal space.
The algorithm adapts to the current spatial scenario. In the SINR sense, it optimally suppresses arbitrary noise and amplifies the desired signal.
Note, that the transform $\mathbf{W}^H$ needs not to track the fast fading, it only depends on the environment. That is, $\mathbf{W}^H$ has to be updated only very seldom. With the WSS assumption $\mathbf{W}^H$ is constant. Hence, the computational complexity is low.
However, the covariance estimation, the EVD and the transform are carried out for each user. Considering a receiver architecture serving a large number of users, this is a critical point.

B. Fixed Beamformer

One of the simplest beamforming techniques is the fixed beamformer [2]. A limited number K_b of static beams is steered in different directions. A popular method is the application of a Buttler matrix at the radio frequency. Without loss of generality, the fixed beamforming is assumed to be a baseband operation. Figure 5 shows an example, where a 6 element uniform linear array (ULA) with $\lambda/2$ element spacing is used to cover a 120^o sector with $K_b = 6$ beams. The beam directions are assumed to be uniformly spaced resulting in the set $\{-50^o, -30^o, -10^o, 10^o, 30^o, 50^o\}$.
Steering fixed beams can be expressed as a $K_b \times K_a$ transform $\mathbf{T}^H$, where the columns of $\mathbf{T}$ are the array response vectors in the look directions of the chosen beams. In the sequel, this transform $\mathbf{T}^H$ is denoted *aperture beam transform* (ABT). It is the core of the fixed beamformer receiver structure in figure 3.
The ABT transforms the aperture signals $\vec{r}(t)$ into the beam domain. For each user the K_f best beam signals are selected and maximum ratio combined.

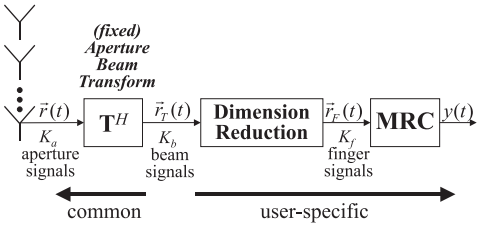

Fig. 3. Fixed Beamformer Receiver Structure

The ABT is performed once for all users. Only the beam selection and the MRC is user-specific. Hence, the complexity of the fixed beamformer is very low. Furthermore, it fits very well to current single antenna receiver concepts.
Comparing figure 2 and figure 3, the fixed beamformer can be considered as a rough approximation of the eigen beamformer. However, $\mathbf{T}^H$ in general does not completely decorrelate the desired and the noise signals. That is, MRC of beam signals is suboptimal. In addition, the SINR concentration usually is lower than in the eigen beamformer, i.e. usually more finger signals are required to determine the signal space.
Nevertheless, section IV shows, that the performance of the fixed beamformer is similar to the eigen beamformer in most scenarios. The fixed beamformer obviously degrades for the following cases:

1. The desired signal impinges between two beam directions. Then, in order to avoid a decreased antenna gain, both adjacent beam signals are selected and MRC combined, although they are highly correlated. This increases the number K_f of finger signals.
2. Strong interferer signals in the vicinity of the desired signal cannot be efficiently suppressed, especially if both are located

in the same beam.

C. Hybrid fixed/eigen Beamformer

In order to benefit at the same time from the low complexity of the fixed beamformer and the high adaptivity of the eigen beamformer, both principles are combined in the following.
From a system theoretical point of view, the beam signals and the aperture signals span the same signal space, as long as the ABT $\mathbf{T}^H$ has full column rank, i.e. $K_b \geq K_a$. That is, applying the eigen beamformer to the beam signals instead of the aperture signals, leads to the same performance as the eigen beamformer. This is done by the hybrid fixed/eigen beamformer depicted in figure 10.
First, the decimator block is ignored, i.e. $\vec{r}_D(t) = \vec{r}_T(t)$. In

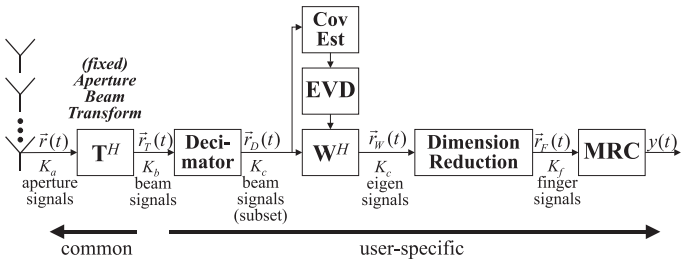

Fig. 4. Hybrid Eigen/Fixed Beamformer Receiver Structure

the first stage, the ABT transforms the aperture signals into the beam domain as in the fixed beamformer. As already mentioned in the previous section, the beam signals $\vec{r}_T(t)$ are not completely decorrelated. The eigen beamformer in the second stage exploits the remaining correlations.
Up to now, the complexity is increased compared with the eigen beamformer due to the additional ABT. However, the complexity can now be strongly reduced by two different steps:

- In scenarios, where the fixed beamformer shows acceptable performance, the decimator and the transform $\mathbf{W}^H$ can be bypassed, i.e. $\vec{r}_W(t) = \vec{r}_T(t)$. This ends up in the fixed beamformer structure shown in figure 3.
- In other scenarios, the ABT $\mathbf{W}^H$ can be considered as a spatial prefilter which to some extend leads to a decorrelation and an SINR concentration. Therefore, the dimension of the signal space can be reduced in the beam domain with only slight performance degradation. This is done by the decimator in figure 4, which selects a K_c-dimensional subset of the K_b beam signals. The covariance estimators, the EVD and the transform $\mathbf{W}^H$ are clearly simplified by this decimation.

Considering such an architecture with a large number of users, each user chooses, depending on its interference scenario, whether to use the bypass mode (equivalent to fixed beamformer) or the hybrid mode, where the decimator (parameter K_c) is adjustable. That is, such an architecture provides a user-specific scalable trade-off between performance and complexity. The eigen beamformer and the fixed beamformer are included as edge points.

III. Simulation Scenarios

The described algorithms are analyzed in section IV by help of link-level simulations under ideal assumptions. Section V compares the beamforming methods under more realistic conditions. The environments for the conducted simulations are presented in the following.

A. Simulation Chain

The simulations are based on the UTRA FDD[2] uplink. Details on this standard are found in [5]. In such a wideband CDMA system with variable spreading factors, challenging interference scenarios are those, where several subscribers use small spreading factors. Here, spreading factor 8 is chosen, which corresponds to a 128kbit/s streaming service.
The channel model is a Rayleigh fading channel with a Jakes Doppler spectrum and a velocity of 120km/h. According to the WSS assumption, no slow-fading is considered. The spatial properties are established as derived in [6].
All signal processing is done on chip-level, i.e. the influence of the chip-filters is not taken into account. Power control is not included.
For the analysis in section IV the channel is frequency-non-selective and constant over one slot ($667\mu s$). The instantaneous channel coefficients as well as the spatial covariance matrices are perfectly known to the receiver.
In secttion V, a more realistic parameter setting is chosen. According to [5], a 4-tap channel with exponential power delay spectrum and 1 chip inter-tap-delay is used. The impulse responses are updated 10 times per slot. The instantaneous channel coefficients are estimated on the received signals by despreading the pilot sequence. The signal covariance matrices are based on the correlation of these coefficients, whereas the interference covariance matrices are computed by correlating the received signal. For the averaging, a slotwise recursive filter with forgetting factor 0.99 is employed. The number of RAKE fingers was limited to 8. Only signals, whose SINR or power, respectively, is larger than 10dB below the best signal are assigned a RAKE finger.
The results are given in terms of raw bit error rates versus E_b/N_0 per receive antenna.

B. Spatial Configurations

For the sake of convenience, only 2 users are simulated[3]. Both are received with the same average power. Three different spatial configurations are chosen and depicted in figure 5. The fixed beams introduced in section II-B are also added.
In the first scenario, the two users are spatially well separated, which usually is a trivial task for beamforming algorithms. In addition, the direction of the desired signal is fully aligned with a beam. The others are worst-cases in the sense of section II-B. Scenario 2 shows two users which are very close to each other within one fixed beam, where the desired user still arrives in the center of a beam. In scenario 3, the desired user impinges

[2] UMTS Terrestrial Radio Access, Frequency Division Duplex Mode
[3] There will not be a large number of high data rate users in a sector. In addition, high data rate users, which are spatially well separated, are shown not to be critical in the next section

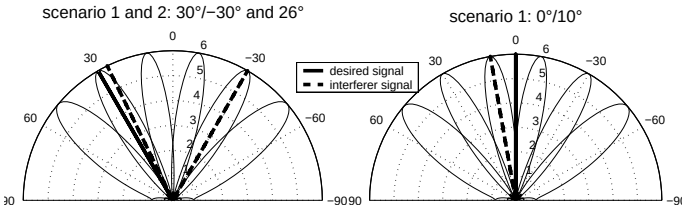

Fig. 5. Simulated 2-user scenarios

	Common	
environment	UTRA FDD uplink	
spreading factor	8	
chip rate	3.84Mchips/s	
carrier frequency	2GHz	
user/interferer power	$\{0dB, 0dB\}$	
fading type	Rayleigh	
Doppler spectrum	Jakes	
velocity	120km/h	
signal DOAs	$\{30^o, 30^o, 0^o\}$	
interferer DOAs	$\{-30^o, 26^o, 10^o\}$	
oversampling	none	
power control	none	
array type	6-ULA $\lambda/2$	
fixed beams	$\{\pm 50^o, \pm 30^o, \pm 10^o\}$	
	Ideal	**Realistic**
angular spread	0^o	5^o
tap delays [chips]	0	$\{0, 1, 2, 3\}$
tap powers [dB]	0	$\{0, -3, -6, -9\}$
channel updates	1 per slot	10 per slot
channel estimation	ideal	real
covariance estimation	ideal	real
RAKE fingers	1(2)	8
RAKE threshold	-	-10

TABLE I
SIMULATION PARAMETERS

from the middle between 2 fixed beams, while the interferer is received from the center of the adjacent beam.
The angular spread of the desired and the interferer signal is 0^o for the analysis and 5^o for the simulations in section V.
The most important simulation parameters are summarized in table I.

IV. ANALYSIS

The environments described in the previous section are now used to analyze and compare the beamforming algorithms, where we make use of the ideal assumptions for the sake of clarity.

A. Eigen Beamformer

The receiver structure of the eigen beamformer was presented in section II-A. The eigen signals $\vec{r}_W(t)$ can be expressed as

$$\vec{r}_W(t) = \mathbf{W}^H \cdot \vec{r}(t) \tag{3}$$

The covariance matrices of the signal and noise component in the eigen domain are

$$\mathbf{R}_{xx}^{(W)} = \mathbf{W}^H \cdot \mathbf{R}_{xx} \cdot \mathbf{W} \quad ; \quad \mathbf{R}_{nn}^{(W)} = \mathbf{W}^H \cdot \mathbf{R}_{nn} \cdot \mathbf{W} \tag{4}$$

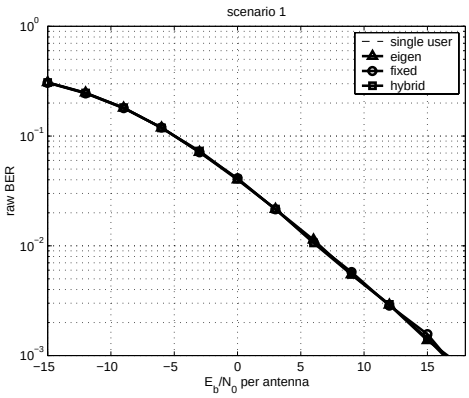

Fig. 6. Ideal Assumptions; Desired signal: 30^o; interferer signal: -30^o

and the SINR γ_i on the eigen signal i is

$$\gamma_i = \frac{\vec{w}_i^H \cdot \mathbf{R}_{xx} \cdot \vec{w}_i}{\vec{w}_i^H \cdot \mathbf{R}_{nn} \cdot \vec{w}_i} \tag{5}$$

where $\vec{w}_i$ is the ith column of the matrix $\mathbf{W}$.
If $\vec{w}_i$ are chosen to be the K_a eigen vectors of the generalized eigen value problem

$$\mathbf{R}_{xx} \cdot \vec{w}_i = \gamma_i \cdot \mathbf{R}_{nn} \cdot \vec{w}_i \tag{6}$$

both covariance matrices in equation (4) become diagonals and each γ_i is maximized [7]. Since an angular spread of 0^o was assumed, the desired signal components $\vec{x}(t)$ of the aperture signals $\vec{r}(t)$ are fully correlated and the SINR is concentrated on only one eigen signal. Hence, $K_f = 1$ finger signal is sufficient to describe the complete signal space.

Figures 6, 7 and 8 depict the bit error performance for the three spatial scenarios. In scenario 1, the two users can be spatially resolved, the interferer can be nulled and the bit error characteristic runs on the single user reference over the complete E_b/N_0 range.
In scenario 2, we have to distinguish between high and low E_b/N_0 ranges. In the low E_b/N_0 region, the interferer is covered by the noise and the bit error characteristic again runs on the single user reference. When the noise level N_0 gets lower, the interferer becomes visible. Then, the eigen beamformer asymptotically nulls this interferer. At the same time, the antenna gain decreases due to the limited spatial resolution and the limited degrees of freedom. Hence, the curve converges towards a shifted version of the single user reference.
For the eigen beamformer, scenario 3 is not of special interest. The spatial resolution of the two users is better than in scenario 2, i.e. the distance to the single user reference in the high E_b/N_0 region is smaller.

B. Fixed Beamformer

In section II-B, the structure of the fixed beamformer was described. Equivalent to the previous section, the beam signals $\vec{r}_T(t)$, the signal and noise covariance matrices $\mathbf{R}_{xx}^{(T)}$ and $\mathbf{R}_{nn}^{(T)}$ and the SINR γ_i on beam i are

$$\vec{r}_T(t) = \mathbf{T}^H \cdot \vec{r}(t) \tag{7}$$

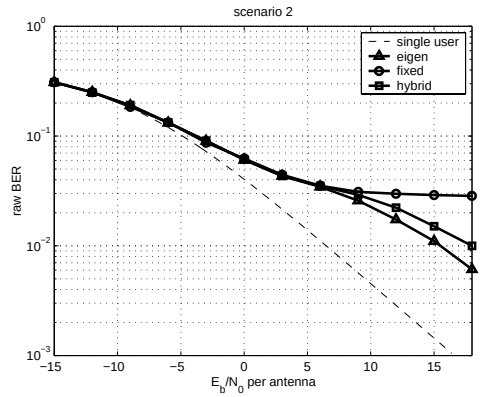

Fig. 7. Ideal Assumptions; Desired signal: 30^o; interferer signal: 26^o

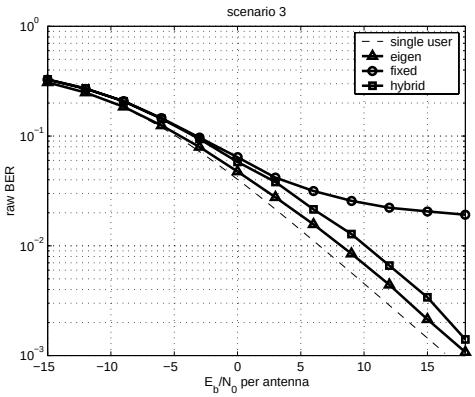

Fig. 8. Ideal Assumptions; Desired signal: 0^o; interferer signal: 10^o

$$\mathbf{R}_{xx}^{(T)} = \mathbf{T}^H \cdot \mathbf{R}_{xx} \cdot \mathbf{T} \quad ; \quad \mathbf{R}_{nn}^{(T)} = \mathbf{T}^H \cdot \mathbf{R}_{nn} \cdot \mathbf{T} \tag{8}$$

and

$$\gamma_i = \frac{\vec{t}_i^H \cdot \mathbf{R}_{xx} \cdot \vec{t}_i}{\vec{t}_i^H \cdot \mathbf{R}_{nn} \cdot \vec{t}_i} \tag{9}$$

where $\vec{t}_i$ is the ith column of the matrix $\mathbf{T}$.
It is obvious, that the covariance matrices in the beam domain in general do not have diagonal structure. Furthermore, the SINR is not maximized, which was the case for the eigen beamformer. Nevertheless, to some extend the ABT provides SINR concentration and decorrelation.
In scenario 1, fixed beamforming leads almost to the same performance as the eigen beamforming in the depicted range. The side lobes of the fixed beams are low, so that signals outside the main lobe are well suppressed.
In scenario 2, the fixed beamforming and eigen beamforming curves also overlap in the low E_b/N_0 region, since again the interferer is covered by the noise. However, in the high E_b/N_0 region the characteristic of the fixed beamformer runs into an error floor, as the interferer cannot be cancelled. In both scenarios, $K_f = 1$ finger signals are sufficient due to the alignment of the signal direction with a beam.
This is not the case for scenario 3. If only one beam signal is selected, the antenna gain would severely degrade (cf. figure 5). Hence, both adjacent beams are chosen ($K_f = 2$). Nevertheless, a loss of approximately 1dB remains[4] in the low E_b/N_0 region. Like in scenario 2, we again see an error floor.

C. Hybrid fixed/eigen Beamformer

The receiver structure of the hybrid technique is explained in section II-C. The $K_b \times K_a$ transform $\mathbf{T}^H$ and the decimator in figure 4 can be summarized to a decimated $K_c \times K_a$ transform $\mathbf{T}_{dec}^H$, where $\mathbf{T}_{dec}$ contains that columns of $\mathbf{T}$ corresponding to the K_c selected beam signals $\vec{r}_D(t)$. Then, the K_c eigen signals $\vec{r}_W(t)$ can be expressed as

$$\vec{r}_W(t) = \mathbf{W}^H \cdot \mathbf{T}_{dec}^H \cdot \vec{r}(t) \tag{10}$$

[4]Due to the increasing beam width at the sector edges, this loss is smaller between the other beams. Other ABT are possible which provide a better sector coverage, e.g. a larger number K_b of beams, wider beams, non-uniformly spaced beams etc.

where $\mathbf{W}^H$ now is a $K_c \times K_c$ transform. The $K_c \times K_c$ covariance matrices estimated on the K_c selected beam signals are

$$\mathbf{R}_{xx}^{(D)} = \mathbf{T}_{dec}^H \cdot \mathbf{R}_{xx} \cdot \mathbf{T}_{dec} \quad ; \quad \mathbf{R}_{nn}^{(D)} = \mathbf{T}_{dec}^H \cdot \mathbf{R}_{nn} \cdot \mathbf{T}_{dec} \tag{11}$$

The EVD operates on these matrices. Equivalent to equation (5), the SINR γ_i an the eigen signal i is

$$\gamma_i = \frac{\vec{w}_i^H \cdot \mathbf{T}_{dec}^H \cdot \mathbf{R}_{xx} \cdot \mathbf{T}_{dec} \cdot \vec{w}_i}{\vec{w}_i^H \cdot \mathbf{T}_{dec}^H \cdot \mathbf{R}_{nn} \cdot \mathbf{T}_{dec} \cdot \vec{w}_i} \tag{12}$$

where $\vec{w}_i$ is the ith column of the matrix $\mathbf{W}$.
In order to cancel a single interfering signal, at least two dimensions are required. Therefore, the decimator is adjusted to select $K_c = 2$ beam signals in all three scenarios, namely the $30^o, 10^o$ directions in the first two scenarios 1 and 2 and the $10^o, -10^o$ directions in scenario 3.
As expected, the differences between this setting and the other methods is negligible in scenario 1. Hence, the hybrid beamformer would choose the bypass mode for users with such interference situations, i.e. it switches to simple fixed beamforming. However, scenario 2 shows the advantage of the hybrid technique. While the fixed beamformer runs into an error floor, the hybrid method exploits the correlation between $K_c = 2$ beam signals in order to asymptotically null the interferer. Like in the eigen beamforming case, the curve converges towards a shifted version of the single user reference. This shift is larger than for the eigen beamformer, since only $K_c = 2$ degrees of freedom are available for nulling (the eigen beamformer uses all $K_a = 6$ degrees of freedom).
In the low E_b/N_0 region of scenario 3, the same degradation as in the fixed beamformer is observed. The reason for that is given in the previous section. The error floor in the high E_b/N_0 region is also avoided here. Due to the better spatial separation, the difference to the eigen beamformer is lower in this scenario. Note, that in contrast to the fixed beamformer, $K_f = 1$ finger signal is sufficient.

V. Simulation Results

In this section, the described methods are compared using a more realistic parameter setting (cf. table I). The spatial scenarios are the same as in the previous section. However, an angular

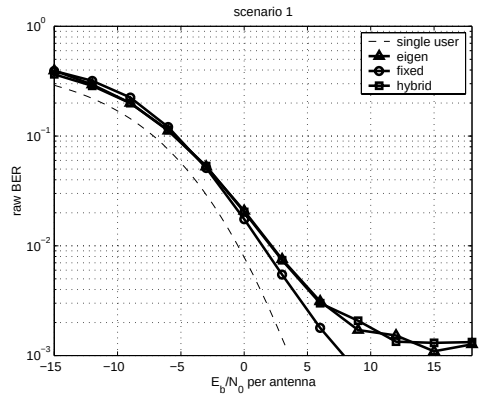

Fig. 9. Realistic Assumptions; Desired signal: 30^o; interferer signal: -30^o

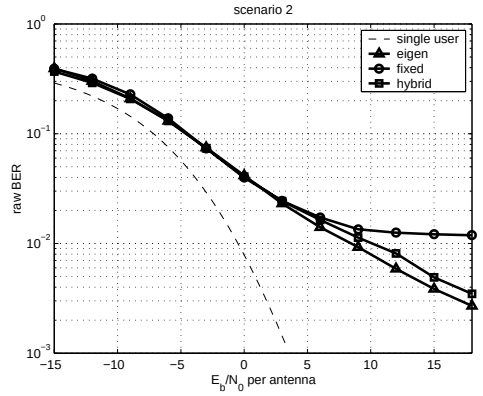

Fig. 10. Realistic Assumptions; Desired signal: 30^o; interferer signal: 26^o

spread of 5^o was considered. The matched filter bound for the employed Rayleigh fading channel [3] is added as a single user reference. The most important differences compared with figures 6-8 are in principle:

- The curves are steeper due to more diversity provided by the channel.
- All curves run into an error floor, since the channel is not constant over one slot.
- Compared with the single user bound, we also get degradations in low E_b/N_0-regions due to noisy channel estimates.

Considering these principle differences, we observe that these results underline the insights discussed in the previous section. Some slight differences are commented in the sequel.
In the simplest scenario 1, the hybrid and the eigen beamformer degrade much more than the fixed beamformer in high E_b/N_0-regions. The reason is, that both try to estimate noise and interference properties. However, their power is very low, so that the relative error due to non-ideal covariance estimation is high. The eigenvalue decompositions suffer from numerical problems in this case.
Another interesting aspect is, that the points, where the curves start to diverge, shift to the right. The non-zero angular spread and the real channel estimation complicate the nulling of the interferer.

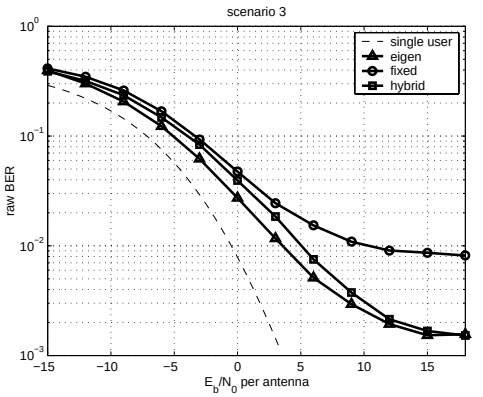

Fig. 11. Realistic Assumptions; Desired signal: 0^o; interferer signal: 10^o

VI. Conclusions

In this article, the simple fixed beamformer and the adaptive eigen beamformer are combined to a hybrid beamforming technique. In this scheme, the eigen beamformer operates on beam signals, which are the output of a fixed beamforming network. As the latter serves as a spatial prefilter, the dimension of the eigen beamformer can be reduced. Hence, the trade-off between performance and complexity can be adjusted for each user separately depending on its effective interference situation.
Simulation results based on the UTRA FDD uplink are presented comparing the hybrid technique with the two stand-alone algorithms. Ideal as well as more realistic parameter settings are taken into account. For spatially separated users, the fixed beamformer achieves almost the same performance as the eigen beamformer over a wide E_b/N_0 range. For such users, the hybrid beamformer chooses the bypass mode, which is equivalent to the simple fixed beamformer structure. If the spatial separation gets worse, the hybrid technique increases the complexity and therewith its adaptivity. By this means, the hybrid method clearly outperforms the fixed beamformer and approaches the performance of the eigen beamformer, whereas the complexity is lower than with the eigen beamformer.

Acknowledgments

The authors would like to thank Dipl.-Ing. Michael Ehler, who did the simulation work presented here throughout his diploma thesis.

References

[1] J.S. Hammerschmidt, C. Brunner, and C. Drewes, "Eigenbeamforming - a novel concept in array signal processing, " *European Wireless 2000*, Dresden, Germany, September 2000.
[2] J. C. Liberti jr. and T.S. Rappaport, *Smart Antennas for Wireless Communications*, Prentice-Hall, 1999.
[3] J. G. Proakis, *Digital Communications*, McGraw-Hill, 1995.
[4] S. Haykin, *Adaptive Filter Theory*, Prentice-Hall, 1996.
[5] 3GPP, *Technical Specification Group Radio Access Network; Spreading and modulation (FDD)*, 3G TS 25.213
[6] I. Viering, R. Reinhardt, T. Frey, "Statistical Modelling of spatially correlated MIMO channels," *ISPACS 2001*, Nashville, November, 2001
[7] C. W. Therrien, *Discrete Random Signals and Statistical Signal Processing*, Prentice-Hall, 1992.